Chemical composition of the lunar surface from neutron leakage fluxes*

CHENG Yu(程宇)[1,2] DONG Tie-Kuang(董铁矿)[1,2;1)] DONG Wu-Dong(董武东)[2]
REN Zhong-Zhou(任中洲)[3,4] XU Ao-Ao(许敖敖)[5]

[1] Space Science Institute, Macau University of Science and Technology, Avenida Wai Long, Taipa, Macau, China
[2] Faculty of Information Technology, Macau University of Science and Technology, Avenida Wai Long, Taipa, Macau, China
[3] Department of Physics, Nanjing University, Nanjing 210008, China
[4] Center of Theoretical Nuclear Physics, National Laboratory of Heavy-Ion Accelerator, Lanzhou 730000, China
[5] Macau University of Science and Technology, Avenida Wai Long, Taipa, Macau, China

Abstract: The neutron leakage fluxes from the lunar surface are calculated by Monte Carlo transport code based on Geant4. The integral fluxes of fast neutrons, epi-thermal neutrons and thermal neutrons are analyzed. Numerical results for 20 kinds of lunar soils and 7 minerals show that the fast neutron fluxes are linearly related to the average atomic mass numbers of the lunar materials used in simulations. Meanwhile, the average atomic mass numbers are strongly modulated by the abundances of iron (Fe) and titanium (Ti), and a linear relationship between the average atomic mass numbers and the abundances of Fe and Ti is found. Furthermore, the results show that the ratios of epi-thermal to thermal fluxes for lunar soils are linearly related to the macroscopic absorption cross sections of lunar materials, and that the macroscopic absorption cross sections monotonically increase with the abundances of Fe and Ti by a simple function. Then we reach the conclusion that the neutron fluxes can provide the information about the Fe and Ti contents.

Key words: neutron leakage flux, Geant4, macroscopic absorption cross section

PACS: 96.12.Kz, 28.20.Gd **DOI:** 10.1088/1674-1137/35/8/007

1 Introduction

In planetary exploration, the distribution of elements on the surface at present is important in understanding the history of formation and evolution of the moon. In order to determine the abundances of elements on the planetary surface, gamma-ray and neutron spectroscopies were proposed and have been used in planetary exploration. Detailed descriptions of the gamma-ray and neutron spectrometers for earlier planetary missions can be found in Refs. [1, 2]. Recent missions of Lunar Prospector [3], Kaguya [4] and Chang'E-1 [5] also carried gamma-ray and/or neutron spectrometers. The gamma-ray and neutron spectrometers have also been widely used to detect the element distribution on other planets, including Mars [6] and Mercury [7]. The underlying physics is as follows. The galactic-cosmic-rays (GCRs) are incident on the surface of a planet with no or little atmosphere, such as the Moon. The GCRs interact with the nuclei of the surface material and produce many secondary particles, such as protons, neutrons, mesons and photons. The charged particles lose energy continually by both electromagnetic and nuclear interactions with the component atoms and nuclei of the lunar surface. The short-lived mesons will decay, for instance, $\pi^0 \rightarrow \gamma + \gamma$. The net result is that the neutrons and gamma-rays dominating the particle fluxes escape from the planetary surface, which can be measured by orbital detectors. In the present work, we put emphasis on the neutrons. Three main interaction mechanisms between neutrons and nuclei will occur: the elastic scattering, inelastic scattering and neutron capture reactions. By elastic scattering, the neutrons will be moderated. The moderating power is determined by the mass and elastic scattering cross

Received 15 November 2010
* Supported by Science and Technology of Development Fund of Macau (042/2007/A3)
1) E-mail: tkdong99@gmail.com

section of the component nuclei. Among the major elements of planet, hydrogen is the lightest, which has a comparable mass with the neutron. Therefore just a little hydrogen can influence strongly the integral flux and shape of neutron spectroscopy. For this reason, neutron spectroscopy can be used to measure the deposition of water on the planetary surface [8–12]. It will also be influenced by neutron capture reactions. According to the very low capture cross section of carbon, neutron spectroscopy can be used to detect the deposition of carbon. For example, it has been used to measure the seasonal change in the CO_2 ice cap on the Mars [13]. In addition, the absorption cross sections for Fe and Ti are larger than other major elements, i.e., O, Na, Mg, Al, Si, and Ca, on the lunar surface. So one can expect neutron spectroscopy also to provide information about the abundances of Fe and Ti. At the same time, the inelastic scattering and neutron capture reactions will produce characteristic gamma-rays of the component nuclei. Therefore, by combining the data of gamma-ray spectroscopy and neutron spectroscopy, one can obtain information about the chemical composition more adequately.

As mentioned above, the interaction processes between the GCRs and nuclei on the planetary surface are very complex. Monte Carlo simulation is the preferred method for these calculations. Monte Carlo methods have been widely used in nuclear radiation detection, more details of which can be found in [14]. Many software based on the Monte Carlo method have been developed and used in various fields. MCNPX [15] and Geant4 [16] have been used in calculating the characteristics of detectors and the neutron and gamma-ray spectroscopies on the planetary surface [4, 17]. In particular, as a free simulation toolkit, Geant4 has been used more and more widely in nuclear physics and techniques (see for example Refs. [18, 19]). In the present work, we will use Geant4 to calculate the neutron fluxes from the lunar surface.

2 Basic physical theory of neutron moderation

In this work, we simulated the neutron fluxes on the lunar surface using Geant4. The galactic-cosmic-rays (GCRs) can penetrate the surface of solid bodies with no or little atmosphere, such as the Moon. Long before GCRs are stopped in the medium, they can induce spallation reactions with the nuclei of surface material and produce many secondary particles. This reaction mechanism can be described by the two-step model, i.e., the knock-on and evaporation process [20]. In the former case, the neutrons are produced with continuous energy up to the incident cosmic-rays. These neutrons can induce further spallation reactions. In the latter case, the neutrons are emitted with energies typically below 10 MeV, and the distribution is Maxwellian. After production, the neutrons will travel in the medium. During transportation, the neutrons will be moderated by elastic scattering and inelastic collision, be absorbed by nuclear reactions, or escape from the surface. The flux and spectroscopy of neutrons are mainly influenced by two factors: the energy loss and the number loss. After elastic scattering against a nucleus with mass number A, the neutron will lose a fraction of its kinetic energy. Since the energy of the neutrons we are interested in is not high, we only consider isotropic scattering. This means that only the s-wave of neutrons scattered by the central field is considered. In this case, the rate of log energy loss is

$$\xi=\ln\left(\frac{E_1}{E_2}\right)=1-\frac{(A-1)^2}{2A}\ln\left(\frac{A+1}{A-1}\right), \tag{1}$$

where E_1 and E_2 are the kinetic energies of the neutron before and after an elastic collision, respectively. From this equation, one can see that ξ is dependent on the mass number of the moderating nucleus but not on the energy. Besides ξ, the moderation power of a given nucleus is also dependent on the elastic scattering cross section σ_s. Therefore, the moderation power of a given nucleus can be described by ξ times σ_s. When the medium includes more than one element, one can define the macroscopic slowing down power

$$\langle\xi\Sigma_s\rangle=\sum_i n_i\sigma_{si}\xi_i, \tag{2}$$

where n_i is the number density of the ith element. The loss of neutrons results from nuclear reactions in which the neutrons are absorbed, such as a thermal neutron capture reaction. Similarly, this process can be described by the macroscopic absorption cross section

$$\langle\Sigma_a\rangle=\sum_i n_i\sigma_{ai}, \tag{3}$$

where σ_{ai} is the thermal neutron absorption cross section for the ith element. When travelling through the lunar surface, the neutrons can be moderated or absorbed, so the moderating ratio is introduced to describe comprehensively the slowing down power of the medium,

$$\eta=\langle\xi\Sigma_s\rangle/\langle\Sigma_a\rangle. \tag{4}$$

As has been pointed out by Feldman et al. [21], the macroscopic slowing down powers $\langle \xi \Sigma_s \rangle$ for lunar samples from Apollo and Luna missions are almost constant. This is because the elements lighter than oxygen in the returned samples are very rare. The main exceptions may be found when H_2O and/or CO_2 are rich. This is because the mass of H is close to that of the neutron, and C has a very low neutron capture cross section. Due to the temperature environment on the lunar surface, H_2O and CO_2 can only exist in the polar regions of the Moon. Since the main purpose of this paper is to investigate the relationship between the neutron fluxes and the major elements of the lunar surface, it is the macroscopic absorption cross section but not the moderating ratio that is considered.

3 The model of simulation

In simulations, the model of the GCR flux (in protons /cm^2/s) is taken as follows [22],

$$J(E,M) = 1.244 \times 10^6 (E+M+x)^{-2.65} \times [E(E+1876)]/[(E+M)(E+1876+M)], \tag{5}$$

where E is the energy (in MeV) of protons, M is the modulation parameter due to the solar activity and $x = 780\ \exp(-2.5 \times 10^{-4} E)$. During periods of maximum solar activity $M = 950$ MeV, and $M = 375$ MeV for minimum activity. The average value during a typical 11-year solar cycle is $M = 550$ MeV. In the present work, we take $M = 550$ MeV. The geometry of the lunar sample is taken to be a sufficiently large cylinder, and the protons incident on the upper surface. In simulations, we take 20 kinds of lunar soils and 7 lunar minerals as materials, the chemical compositions of which are shown in Table 1. The minerals used for simulation are $Ca_2Si_2O_6$, $CaMgSi_2O_6$, $CaFeSi_2O_6$, $Fe_2Si_2O_6$, $CaAl_2Si_2O_8$, $K_2Al_2Si_2O_8$, Fe_2SiO_4. The data for these materials are taken from Ref. [23]. Obviously, the density of lunar soils and minerals is dependent on the average atomic mass number and the total number of atoms per volume. Therefore, it is difficult to determine the density of lunar soils beforehand. For this reason, we keep the density and geometry parameters of materials as constants. The mass of the materials is

$$m = \nu \langle A \rangle = \rho V, \tag{6}$$

where $\langle A \rangle$ (in gram/mol) is the average atomic mass per mole and ν is the total mole number of atoms. The average atomic mass per mole is

$$\langle A \rangle = \sum_i f_i A_i. \tag{7}$$

In this equation, f_i is the number fraction of the ith element. Then the total mole number of atoms per volume is

$$\frac{\nu}{V} = \frac{\rho}{\langle A \rangle}. \tag{8}$$

Table 1. Composition of 20 kinds of lunar samples from Apollo (A) and Luna (L) missions [23].

mission	SiO_2	TiO_2	Al_2O_3	FeO	MnO	MgO	CaO	Na_2O	K_2O	Cr_2O_3	P_2O_5	S
A11	42.0	7.5	13.5	15.8	0.21	7.9	12.0	0.44	0.14	0.30	0.10	0.11
A12	46.1	2.7	12.6	16.5	0.21	10.2	10.3	0.46	0.24	0.38	0.30	0.08
A12	47.0	2.5	14.3	14.6	0.20	9.1	10.6	0.64	0.39	0.33	0.39	0.07
A14	47.7	1.7	17.4	10.5	0.14	9.4	10.9	0.70	0.52	0.20	0.49	0.10
A15	46.2	2.0	10.4	19.8	0.25	11.1	9.6	0.30	0.094	0.53	0.11	0.06
A15	46.3	1.3	15.6	13.0	0.17	11.9	10.4	0.41	0.16	0.36	0.16	0.07
A15	46.7	1.5	16.4	12.2	0.16	10.4	11.2	0.46	0.21	0.34	0.22	0.08
A15	46.5	1.3	17.6	11.6	0.16	10.4	11.5	0.42	0.18	0.31	0.16	0.07
A16	44.9	0.59	26.7	5.44	0.07	6.0	15.3	0.46	0.121	0.111	0.12	0.07
A16	45.0	0.66	26.2	5.85	0.07	6.3	15.1	0.46	0.131	0.119	0.14	0.08
A16	45.3	0.50	28.3	4.36	0.06	5.0	15.9	0.48	0.083	0.084	0.10	0.0
A16	45.3	0.47	28.0	4.45	0.06	5.4	16.4	0.46	0.107	0.086	0.11	0.05
A16	44.7	0.39	28.7	4.14	0.05	4.6	16.3	0.53	0.084	0.080	0.08	0.03
A17	38.7	8.8	6.5	22.3	0.29	14.5	7.5	0.37	0.077	0.70	0.06	0.05
A17	39.9	9.6	10.9	17.7	0.24	9.5	10.7	0.38	0.078	0.46	0.07	0.12
A17	43.5	3.3	18.2	10.7	0.15	10.8	12.2	0.40	0.116	0.28	0.09	0.08
A17	45.1	1.3	21.3	8.3	0.11	9.8	12.9	0.43	0.144	0.22	0.13	0.06
L16	44.3	3.4	15.6	16.3	0.21	8.4	11.9	0.39	0.11	0.30	0.05	0.21
L20	45.2	0.49	22.8	7.3	0.11	9.5	14.4	0.35	0.07	0.19	0.12	0.0
L24	44.8	1.1	11.8	19.7	0.26	9.7	11.3	0.28	0.03	0.46	0.04	0.14

When the flux of the GCRs is fixed, the number of GCR-induced nuclear interactions and hence the neutron leakage fluxes are proportional to the atom number density of the material. Therefore we multiply the calculated fluxes by the factor $\langle A\rangle/\rho$, e.g., $J_{\text{fast}}\langle A\rangle/\rho$ (in neutrons · cm/s), which are independent of the density of the lunar soils.

4 Numerical results and analysis

Now, let us analyze the neutron fluxes in different energy ranges, i.e., the fast neutron with energy between 0.6 MeV and 8 MeV, the epi-thermal neutron with energy between 0.4 eV and 0.6 MeV, and the thermal neutron with energy less than 0.4 eV. We choose 20 kinds of typical soils and 7 minerals as materials to simulate the neutron leakage fluxes from the lunar surface. The compositions of lunar soils are listed in Table 1. It is reasonable to believe that the conclusions drawn from the results for these materials can be applied to others. According to the above discussions, the fast neutrons are mainly produced by GCR-induced spallation reactions. One can expect that the number of fast neutrons will increase with the neutron numbers in the nuclei of materials. The major components of the Moon are stable light nuclei, among which Fe and Ti are the heaviest ones. For these nuclei, the neutron number and proton number tend to be equal. So the fast neutron flux will be related to the average atomic mass of the material. From Table 1, one can see that the contents of FeO in different samples range from 4.14% to 22.3%, and that the contents of TiO_2 range from 0.39% to 9.6%. So the abundances of them will influence the average atomic mass strongly. Now let us investigate the quantitative relationship between the fast neutron flux and the average atomic mass. The main purpose of choosing these minerals is to extend the range of the average atomic mass. The average atomic masses of the returned lunar samples change in a small range, typically from 21 to 24. As discussed in Sec. 3, the neutron flux is related to the density of the material, so we multiply the flux by a factor $\langle A\rangle/\rho$. The results are shown in Fig. 1. From this figure, one can see immediately that the fast neutron fluxes are linearly related to the average atomic mass. The relationship is given by

$$J_{\text{fast}}\langle A\rangle/\rho = a\langle A\rangle - b, \tag{9}$$

where $a = 0.612$ and $b = 1.787$. The linear relationship between the fast neutron fluxes and the average mass number has also been obtained by Gasnault et al. [24]. The difference is that in Ref. [24] they do not consider evidently the dependence of the neutron fluxes on the density of the lunar soils. The present work can be regarded as a natural extension of Ref. [24]. It must be noted that this relationship is valid for typical minerals and soils. It will be modified strongly when element H is abundant. Then let us see the dependence of the average atomic mass on the abundance of Fe and Ti. From Fig. 2, we can see clearly that the average atomic mass is also linearly related to the mole percentage of iron and titanium. Then one can reach the conclusion that the fast neutron flux is related to the mole percentage of Fe and Ti linearly.

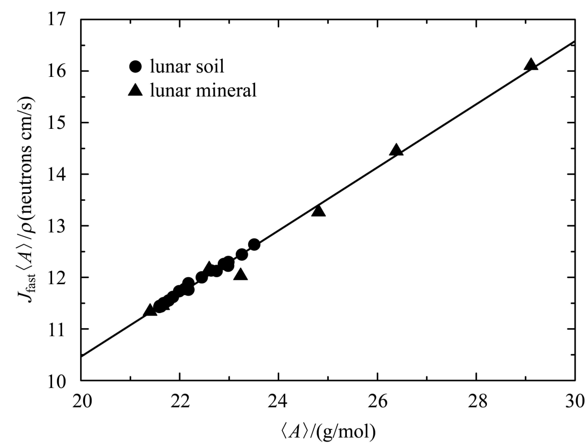

Fig. 1. The simulated fast neutron leakage flux $J_{\text{fast}}\langle A\rangle/\rho$ (in neutrons · cm/s) from the lunar surface for 20 kinds of soils from Apollo and Luna missions and 7 lunar minerals. The composition of the materials is taken from Ref. [23].

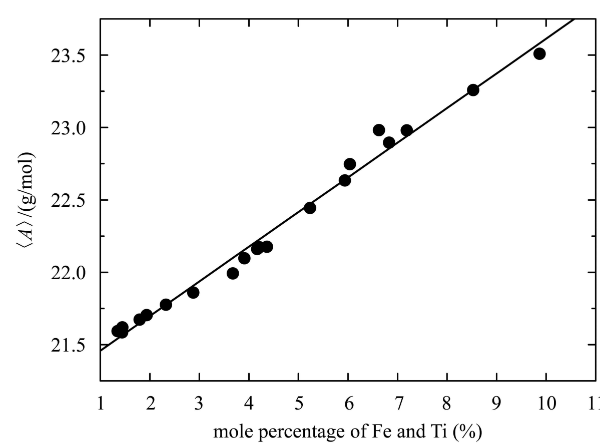

Fig. 2. Average atomic mass of 20 kinds of lunar soils versus the mole percentage of iron (Fe) and titanium (Ti).

Besides the largest mass number, Fe and Ti have much larger thermal neutron absorption cross sections than other major elements on the lunar surface. Now let us investigate the relationship between the macroscopic absorption cross section and the contents of iron and titanium. When neutrons are transporting in the lunar surface, they will either be scattered to lower energies or be absorbed. According to the neutron transport theory, the ratio of epi-thermal to thermal fluxes is linearly related to the parameter $\langle \Sigma_a \rangle / \langle \xi \Sigma_s \rangle$ [21]. Since the macroscopic slowing down powers are almost constant for typical lunar soils, for which elements H and C are very rare, we only show the ratios of epi-thermal to thermal neutron fluxes versus the macroscopic absorption cross section in Fig. 3. The data of thermal neutron absorption cross sections are taken from Ref. [25]. From this figure, one can see that the ratio $J_{\text{epi.}}/J_{\text{therm.}}$ does relate to $\langle \Sigma_a \rangle$ linearly,

$$J_{\text{epi.}}/J_{\text{therm.}} = 2.432 + 200.61 \langle \Sigma_a \rangle. \tag{10}$$

This means that the simulated results are fairly consistent with the neutron transport theory. Then it is interesting to see whether there are simple relationships between the macroscopic absorption cross sections and the mole percentages of Fe and Ti. In Fig. 4, we show the macroscopic absorption cross sections for 20 kinds of lunar soils versus the mole percentage of iron and titanium. From this figure, one can see that the macroscopic absorption cross sections monotonically increase with the increasing contents of Fe and Ti, and that the relationship deviates from the linear function slightly.

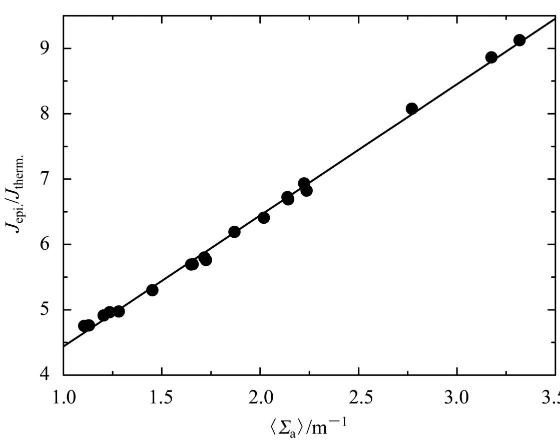

Fig. 3. The relationship between the ratio of epi-thermal to thermal neutron fluxes $J_{\text{epi.}}/J_{\text{therm.}}$ and the macroscopic absorption cross sections for 20 kinds of soils.

Combining the results given above, one can reach the conclusion that the neutron fluxes in different energy ranges can be used together to derive the abundance of Fe and Ti. In principle, it is possible to obtain the abundance of one of these two elements when the other one can be constrained by other tools. For example, if the abundance of Fe can be determined using, for instance, orbital gamma-ray spectroscopy or the optical spectral reflectance one can obtain the abundance of Ti.

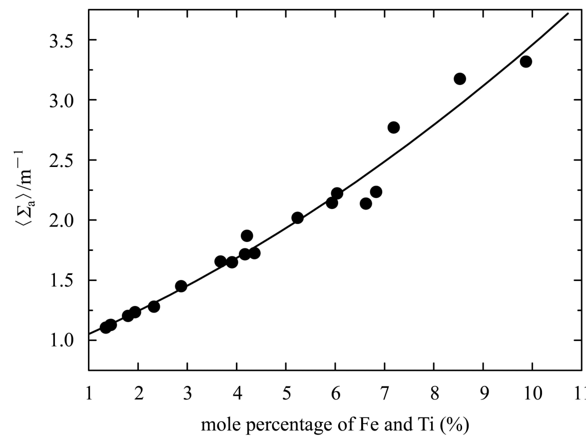

Fig. 4. Macroscopic absorption cross sections for 20 kinds of lunar soils versus the mole percentage of iron (Fe) and titanium (Ti).

Finally, it should be noted that in the above discussions, H, C and the Rare Earth Elements (REEs) are assumed to be ignored. In theory, hydrogen will strongly modify the relationship between the fast neutron fluxes and the average atomic mass. In addition, the macroscopic slowing down power will increase sharply when the content of element H increases [21] and the macroscopic absorption cross section will be modified strongly when C is rich. For these cases, the moderating ratio but not the macroscopic absorption cross section will be used to analyze the ratio of epi-thermal to thermal neutron fluxes. Furthermore, the REEs Gd and Sm are very strong thermal neutron absorbing elements. The macroscopic absorption cross section will be modified strongly with quite small REEs. So in order to obtain the abundance of Fe and Ti as accurately as possible, it is necessary to determine the abundance of REEs by the relationship with Th [23]. The content of Th can be measured by gamma-ray spectroscopy [4].

5 Summary and discussion

In summary, the neutron leakage spectroscopy above the lunar surface has been simulated by Geant4. In calculations, 20 kinds of typical lunar soils and 7 minerals are used as materials. The neutron fluxes in different energy ranges have been analyzed in terms of the chemical composition of the lunar surface. It is found that the fast neutron fluxes are linearly related to the average atomic masses and the ratios of epi-thermal to thermal fluxes are linearly related to the macroscopic absorption cross sections. By further analysis, we find that the average atomic masses and the macroscopic absorption cross sections are modulated strongly by the abundances of Fe and Ti elements when light elements H and C are absent. The linear relationship between the average atomic masses and the mole percentage of Fe and Ti for 20 kinds of lunar soils is found. The dependence of macroscopic absorption cross sections on the abundances of Fe and Ti are also investigated. It is found that the macroscopic absorption cross sections monotonically increase with the abundances of Fe and Ti by a simple function. The reason for these results is that both the masses and the thermal neutron absorption cross sections for Fe and Ti are larger than other major elements on the lunar surface. Then we draw the conclusion that the abundances of Fe and Ti can be derived by analyzing the neutron fluxes of different energy ranges. However, it should be pointed out that the accurate absolute neutron fluxes on the lunar surface are difficult to obtain. For instance, the error bars in the average masses of lunar materials derived from the neutron fluxes measured by the orbital detector of the Lunar Prospector are quite large (about 0.5) [24]. So the calculated fluxes cannot compare directly with the experimental data at present. It is expected that more accurate data will be obtained when the detectors land on the lunar surface. Even so, theoretical calculations can provide useful references for data analysis.

References

1 Evans L G, Reedy R C, Trombka J I. Introduction to Planetary Remote Sensing gamma Ray Spectroscopy. In: Pieters C M, Englert P A J ed. Remote Geochemical Analysis: Elemental and Mineralogical Composition. Camberidge: Camberidge Unversity Press, 1993. 167

2 Feldman W C, Boynton W V, Drake D M. Planetary Neutron Spectroscopy from Orbit. In: Pieters C M and Englert P A J ed. Remote Geochemical Analysis: Elemental and Mineralogical Composition. Camberidge: Camberidge Unversity Press, 1993. 213

3 Feldman W C et al. Nucl. Instrum. Methods in Phys. Res. A, 1999, **422**: 562

4 Kobayashi S et al. Space Sci. Rev., 2010, **42**: 347

5 MA Tao et al. Advances in Space Research, 2008, **154**: 193

6 Feldman W C et al. Science, 2002, **297**: 75

7 Mitrofanov I G et al. Planetary and Space Science, 2010, **58**: 116

8 Boynton W V et al. Science, 2002, **297**: 81

9 Mitrofanov I G et al. Science, 2002, **297**: 78

10 Lawrence D J et al. Science, 1998, **281**: 1484

11 Feldman W C et al. Science, 1998, **281**: 1489

12 Feldman W C et al. Science, 1998, **281**: 1496

13 Prettyman T H, Feldman W C, Titus T N. J. Geophys. Res., 2009, **114**: E08005

14 XU Shu-Yan. Monte Carlo Methods and Their Applications to Experimental Nuclear Physics. (Revised). Beijing: Atomic Energy Press, 2006. 1 (in Chinese).

15 https://mcnpx.lanl.gov/

16 Agostinelli S et al. Nucl. Instrum. Methods in Phys. Res. A, 2003, **506**: 250

17 Lawrence D J et al. J. Geophys. Res., 2006, **111**: E08001

18 SONG Yu-Shou, YE Yan-Lin, GE Yu-Cheng et al. Chinese Physics C, 2009, **33**: 860

19 ZHANG Yi, ZHANG Xiao-Dong, WANG Wen-Xin et al. Chinese Physics C, 2009, **33**: 42

20 Serber R. Phys. Rev., 1947, **72**: 1114

21 Feldman W C et al. J. Geophys. Res., 2000, **105**(E8): 347

22 Reedy R C. J. Geophys. Res., 1987, **92**: E697

23 Lucey P. Reviews in Mineralogy and Geochemistry, 2006, **60**: 83

24 Gasnault O et al. J. Geophys. Res., 2001, **28**(19): 3797

25 Baum M, Knox H D, Miller T R. Chart of the Nuclides (Sixteen Edition), 2002. 40